Design of a Reverse-electrowetting Transducer Based Wireless Self-powered Motion Sensor

Nishat T. Tasneem[1], Dipon K. Biswas[1], Pashupati R. Adhikari[2], Russell Reid[3], Ifana Mahbub[1]
[1]Department of Electrical Engineering, University of North Texas, Denton, TX, USA.
[2]Department of Mechanical and Energy Engineering, University of North Texas, Denton, TX, USA.
[3]Department of Mechanical Engineering, Dixie State University, St. George, Utah, USA

***Abstract*—This paper presents a self-powered motion sensor based on reverse-electrowetting on dielectric (REWOD) energy harvesting having the capability of remotely keeping a track of any motion activity. The energy harvester includes a rectifier and a voltage regulator to provide the DC supply voltage to the analog front-end and the transmitter to wirelessly transfer the data from the motion sensor. The on-chip circuitry includes a seven-stage voltage-doubler based rectifier, an amplifier, an analog-to-digital converter (ADC), and a transmitter, and is designed in standard 180 nm CMOS process with a supply voltage of 1.8 V. The recycled folded cascode (RFC) based charge amplifier has a closed-loop gain of 53 dB within the bandwidth of 1-150 Hz, which is suitable to detect any low-frequency motion signal. An 8-bit SAR-ADC is designed to digitize the amplified signal with a sampling rate of 1 ksamples/s. The transmitter used for this application operates in the 3.1-5 GHz frequency band with an energy efficiency of 8.5 pJ/pulse at 100 kbps data rate. The wireless motion sensing device with the REWOD can be suitable for quantitatively monitoring the motion-related data as a wearable sensor.**

***Index Terms*—Self-powered, reverse-electrowetting energy harvesting, motion sensor, CMOS, recycled folded cascode amplifier, SAR-ADC, IR-UWB, schottky diode.**

I. Introduction

With the promising development in the healthcare industry, extensive research has been carried out in the areas of sensors to remotely monitor healthcare activities. In an approach to eliminate the need of periodic battery replacement and maintenance, wearable and self-powered sensors have attracted a great deal of attention. Energy harvesting is basically the process of transducing ambient kinetic or mechanical energy that surrounds us all the time into electrical energy [1]. The energy sources could be of various forms such as: heat, light, pressure, vibration, electrostatic, and sound, to be harnessed for the sustainable driving of the wearable medical devices [2]. Recently, an electrostatic energy harvesting technique called triboelectricity has been introduced that can operate at various frequencies with high power output [3]. However, the triboelectric generators have a short life-span due to the continuous friction between the electrodes, thus decaying the energy efficiency. Flexible, fiber-based energy harvesting generators (FBG) that converts the bio-mechanical vibration energy to electrical energy, involving conducting fibers integrated into clothing have been proposed in [4]. The current generation in FBG is too low (typically $\sim$ 0.1 $\mu W/cm^2$) to reliably power medical devices. Misra *et al.* have developed transducers utilizing nanotechnology to maximize power density using body heat through flexible materials while simultaneously minimizing the power consumption by incorporating CMOS circuitry working in the sub-threshold region and ultra-low-power radios [5]. With the miniaturization of electronic devices that need to be integrated with energy harvesters to power wearable sensors, energy density is a key factor to power these sensors. Owing to the limitations of various energy harvesters that could potentially power wearable sensors in health monitoring, new approach in energy harvesting based on mechanical motion of liquid electrolyte between the electrodes to generate alternating current has been surfaced and is known as reverse electrowetting on dielectric (REWOD) energy harvesting [6]. REWOD has been demonstrated to generate very high power densities at low driving frequencies compared to the conventional kinetic energy harvesters [6]. Since many energy harvesters operate at a fairly high resonant frequency, they cannot be used in motion activity detection sensors that require to be operated at low frequency ($<$10 Hz). As can be seen from Fig. 1, the harnessed power from a REWOD generator due to various low-frequency movements such as walking and running can provide power to the CMOS Integrated Circuit. The energy harvesting circuit typically includes a rectifier for the AC-DC power conversion and a DC-DC converter for the supply voltage regulation. As the sensor front-end circuit, an amplifier is designed to amplify the generated electrical signal by the transducer, followed by an analog-to-digital converter to digitize the signal and a transmitter circuitry to transmit the sensed signal wirelessly to a remote receiver.

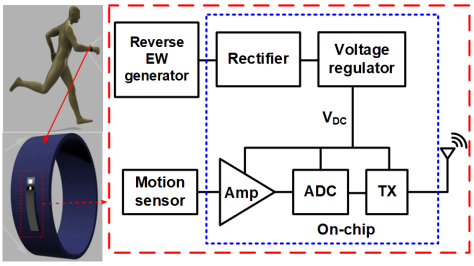

Fig. 1. On-chip front-end motion sensor with the energy harvester.

A rectifier with the capability to rectify a low input power is one of the most desirable units in energy harvesting circuit for low power wireless sensors [7]. However, the conventional diodes require $\sim$0.7 V of input forward-bias voltage which limits the operation of the rectifier [8]. A better approach is to

use a schottky diode based rectifier due to the low forward-bias voltage requirements of the schottky diode [9]. In the sensor front-end circuitry, several architectures of the charge amplifier have been proposed in the literature. In order to improve the transconductance, DC gain, and input-referred noise performance of the conventional FC-OTA, current reusing technique is introduced [10]–[14]. As the charge amplifier is required to have a high gain (>40 dB) depending on the transducer's charge generation with very low power consumption (<2 μW) for biomedical applications, the designed OTA in this work utilizes the recycling folded-cascode (RFC) technique [15]. With the enhancement in transconductance, the amplifier could be prone to instability as the phase-margin could be reduced. The proposed architecture of the fully-differential charge amplifier also enhances the phase-margin as well as reduces the input-referred noise, thus making the system stable. In order to digitize the amplified signal, a successive approximation register-ADC (SAR-ADC) has been the most widely used architecture for its low-power consumption at a low sampling rate [16], making it suitable for low-frequency biomedical sensor applications. This paper presents an SAR-ADC based on the charge redistribution network with a target of maintaining low-power operation. At the transmitting end, impulse radio ultra-wideband (IR-UWB) transmitter is the most suitable for low-power application. By using duty-cycled IR-UWB transmitter, the system can maintain a strict power budget [18]. The transmitter also needs to comply with the spectrum regulation imposed by the Federal Communication Commission (FCC) for UWB communication which requires the peak power spectral density to be lower than -41.3 dBm/MHz [19].

The contributions of this paper is as follows: (a) Modeling and fabrication of a REWOD based energy harvester that can harvest 20-90 nA_{pp} of current at a frequency range of 1-10 Hz, (b) an on-chip charge amplifier with 53.7 dB gain, (c) a 7-stage schottky diode based rectifier which achieves a maximum power conversion efficiency (PCE) of 62%, (d) an 8-bit SAR ADC, and (e) an IR-UWB transmitter with reconfigurable frequency and bandwith features working in the 3.1 to 5 GHz frequency band. Section II presents the description of all the blocks, section III shows the simulation results, and a concluding remark is presented in section IV.

II. Overview of the Self-powered Motion Sensor

A. Reverse Electrowetting on Dielectric Energy Harvester

REWOD energy harvesting is the opposite to electrowetting operating at low-frequency range [20], [21]. In its simplest form, REWOD involves a conductive droplet being repeatedly squeezed between two electrode substrates. This results in a modulating electrical double layer (EDL) capacitance. The AC current generation due to the EDL capacitance change is shown in Fig. 2. The amount of current generated by the fabricated REWOD-transducer depends on the contact surface area between the conductive liquid (e.g. $NaCl$ solution) and the electrodes, which is correlated to the displacement. The bottom electrode is a multilayer structure with Aluminum

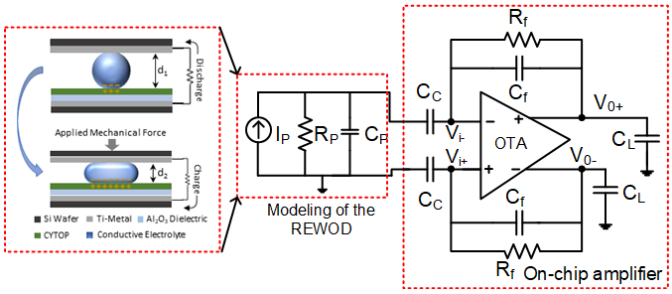

Fig. 2. Modeled reverse electrowetting energy harvester with amplification.

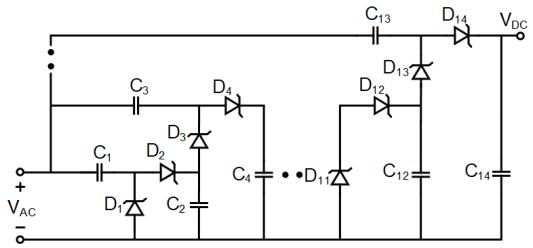

Fig. 3. Proposed seven-stage Schottky diode based rectifier circuit.

Oxide (Al_2O_3) as the dielectric and CYTOP solution as the hydrophobic material. CYTOP is an amorphous fluoropolymer that not only makes the surface hydrophobic, but also acts as a secondary layer of dielectric in addition to Al_2O_3. As an initial approach to verify the phenomenon, the displacement between the top and bottom electrode is mechanically varied, thereby changing the contact surface area at certain input frequency. The fabricated device is modeled as an AC current source (I_p) with a parallel resistor (R_p) and a capacitor (C_p) as shown in Fig. 2. The average value of R_p and C_p is measured using the CHI600E potentiostat and found to be 7.44 MΩ and 94.6 nF, while I_p is in the range of 25 - 90 nA_{p-p}.

B. Rectifier Circuit

The proposed rectifier circuit is a seven-stage voltage-doubler circuit. It is designed using schottky diodes due to the low forward-bias voltage of the schottky diode architecture. A voltage doubler circuit consists of two diodes D_1, D_2 and two capacitors C_1 and C_2 as shown in Fig. 3 [22]. The architecture works as a full wave rectifier where D_1 operates during positive half cycle and D_2 operates during the negative half cycle of the input AC signal. The capacitor values are chosen to be 100 pF to produce a smoother DC signal at the output. The proposed seven-stage voltage doubler circuit is designed so that it can rectify as low as 100 mV input voltage.

C. Charge Amplifier

The change in motion-dependent surface charge density due to the mechanical vibration of the conductive liquid in the REWOD transducer can be converted to a proportional voltage signal by the charge amplifier. The charge amplifier includes an OTA, a input capacitor (C_C) and the capacitive feedback loop (R_f and C_f) in a fully differential structure as shown in Fig. 2. The amplifier produces a voltage across C_f, which is proportional to the generated charge. The input impedance of

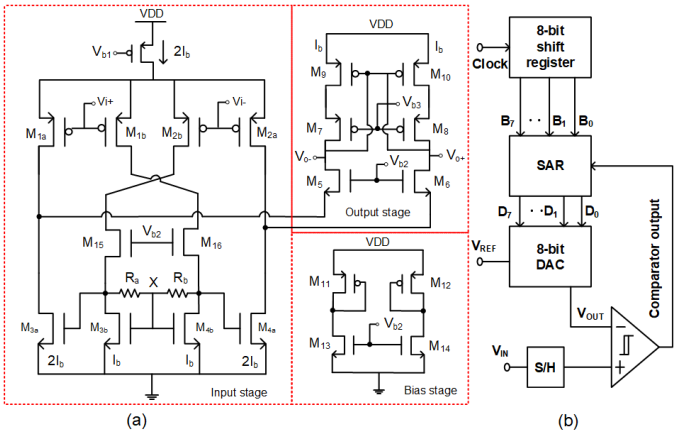

Fig. 4. (a) Schematic of the recycled folded-cascode OTA, (b) Block diagram of the SAR-ADC.

the charge amplifier is designed to be almost zero so that most of the current is passed through the amplifier. Keeping all these design constraints into consideration, the charge amplifier is designed with a folded-cascode OTA with current recycling technique to have a high gain-bandwidth-product (GBW), low power consumption, and a high signal-to-noise ratio as shown in Fig. 4(a). As the gain depends on the product of the output impedance (R_o) and the transconductance (G_m) [10], the input pair transistor of the conventional FC is split into two pairs: M_{1a}-M_{1b} and M_{2a}-M_{2b} in order to split the current from $2I_b$ to I_b. In this work, pMOS transistors are used as the input pair as this can reduce the flicker noise components compared to the nMOS transistors. The bottom transistors are also split into M_{3a}-M_{3b} and M_{4a}-M_{4b} to operate as the common-mode feedback current mirror along with the equal resistors R_a and R_b [15]. Since the node 'X' (Fig. 4(a)) is floating, no current goes through the resistors. G_m of the proposed OTA can be expressed as follows:

$$G_m = 2(1 + g_{m,3a}R_a)g_{m,1a} \tag{1}$$

where $g_{m,3a}$ and $g_{m,1a}$ are the transconductances of the transistors M_{3a} and M_{1a}, respectively. As the gain largely depends on R_a, its value is chosen as 25 kΩ to meet high open-loop gain specification. The current through the tail transistors (M_{3a}/M_{3b}) depends on the aspect ratio (W/L) of them. At the output stage, M_5-M_6 pair is sized as the transistors M_{15}-M_{16} to have the same biasing. The bias voltages V_{b2} and V_{b3} are chosen to have the output current as I_b. Thus, the total bias current sums up to be $6I_b$. To reduce the power consumption of the OTA, I_b is chosen to be 200 nA.

D. ADC

The 8-bit ADC is designed with a switched capacitor architecture based on charge redistribution logic as shown in Fig. 4(b). It includes a shift register, an SAR logic circuit, an 8-bit digital-to-analog (DAC) converter, a sample-and-hold circuit, and a comparator. The ADC is designed to have a low-power consumption and a sampling frequency of 1 ksamples/s, as the motion sensing signals would lie in a low-frequency bandwidth (typically 0.1 to 10 Hz).

E. Transmitter

The proposed IR-UWB transmitter circuit consists of an impulse generator (IG), a voltage controlled oscillator (VCO) and a power amplifier (PA) as shown in Fig. 5. The proposed transmitter is designed to transmit digitized sensed signal with 100 kbps data rate. The details of the blocks are described below:

1) Impulse Generator: The impulse generator is designed using a current-starved inverter based delay circuit where the output pulse V_{delay} of the delay circuit is controlled using an external control voltage V_c. The circuit is made of two-stage cascaded inverter circuit using pMOS and nMOS transistors. The delay circuit is followed by an inverter, a NAND gate and an inverter to generate the impulse signal which is used for duty-cycling the VCO and the PA.

2) Voltage Controlled Oscillator: The voltage controlled oscillator is a complementary cross-coupled LC-VCO having two pMOS and two nMOS transistors. The W/L ratio of the transistor M_7-M_9 and M_8-M_{10} are set in such a way to operate in the strong inversion region to ensure high G_m. The LC tank of the VCO includes an inductor, L of 2.7 nH and a varactor pair, C_{VAR} which achieves a capacitance in the range of 4.5 – 17 pF for the control voltage, V_{ctrl} of 100 mV to 1.8 V range. The varactor pair is used to achieve the oscillation frequency f_0 in the range 3.5 - 5 GHz with the total capacitance, C= $C_{VAR} \parallel C_b \parallel C_{gd,M8} \parallel C_{gd,M9}$. At the output of the VCO, a 300 fF DC blocking capacitor, C_b is also used to block the DC components of the generated RF signal. The tail current source of the VCO is actually a current mirror formed by transistor M_{12} and M_{13}. To duty-cycle the VCO, the pulse signal generated by the impulse generator is used at the gate of the transistor M_{11} that turns on and off the tail current source of the VCO.

3) Power Amplifier: The proposed differential class E power amplifier includes a choke inductor pair L_1-L_2 and two cascoded nMOS transistors in each branch. Optimum sizes of the transistors are chosen to have small on-resistance and small parasitic capacitance. The PA is duty-cycled using the pulse signal V_{VCO} at the gate of the transistors M_{14} and M_{15}. The differential output signal of the VCO is provided to the gate of M_{16} and M_{17}. To feed the differential output of the PA to the single-ended antenna, a matching network and a balun is used after the PA.

III. Simulation and Measurement Results

The power conversion efficiency (PCE) of the proposed rectifier is shown in Fig. 6(a) for the input voltage range of 100 mV to 1.4 V. The maximum PCE is simulated to be 62% with the load resistance R_L as 1 $M\Omega$. The measured harvested DC power from the motion sensor after the single-stage rectification is presented in Fig. 6(b). As the REWOD transducer is modulated from 1.5 mm to 4 mm displacement, the generated DC power increases over the motion frequency. Fig. 7(a) presents the closed-loop gain of the charge amplifier as 53.7 dB. As the gain depends on the ratio of the input and feedback capacitances, the values of them are chosen as

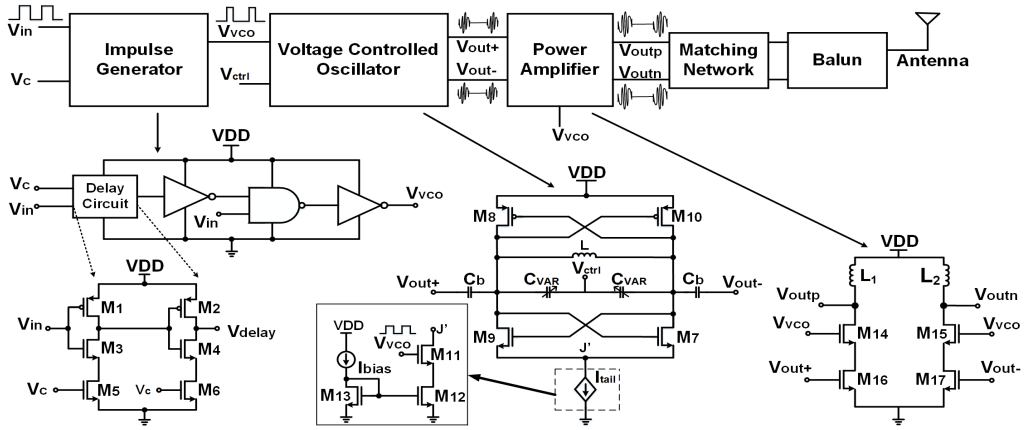

Fig. 5. Schematic of the proposed transmitter circuit.

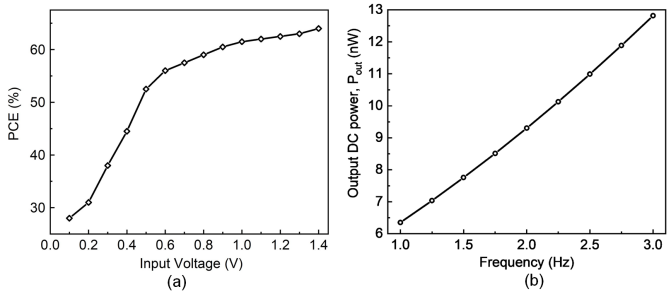

Fig. 6. (a) Power conversion efficiency of the rectifier, (b) measured output DC power over motion frequency.

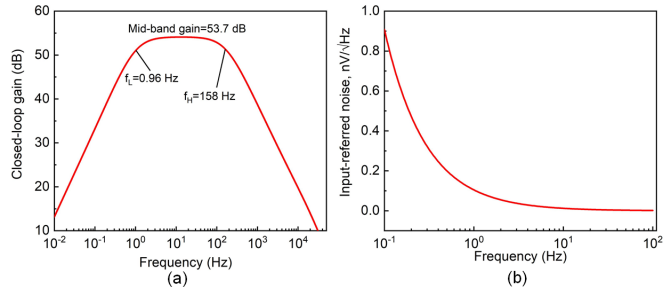

Fig. 7. (a) Closed-loop gain, (b) noise performance of the amplifier.

1 nF and 2 pF, respectively. The feedback resistor is designed to maintain the lower cut-off freqeuncy at ∼1 Hz. Since the motion sensor is designed to detect low-frequency signal, the higher cut-off frequency is kept as ∼150 Hz. The total bias current is 1.2 μA in order to reduce the power consumption to 2.35 μW. The noise performance is shown in Fig. 7(b). The input-referred noise is 3.8 μV_{rms} integrated over 1 to 200 Hz frequency band. After the amplification, the ADC converts the analog voltage signal to 8 digital bits at 1 ksamples/s with a total power consumption of 277 μW, and effective number of bits of 6.8.

An impulse signal of 1.8 V is generated with a pulse width of 5 ns for 100 kbps data rate when the control voltage V_c is 600 mV and consumes 800 pW power for 1.8 V supply voltage. Varying the control voltage V_c from 100 mV to 600 mV, the pulse width of the impulse signal can be varied as high as 10 μs to 720 ps respectively which enables a reconfigurable bandwidth of 500 MHz - 1.39 GHz. Varying

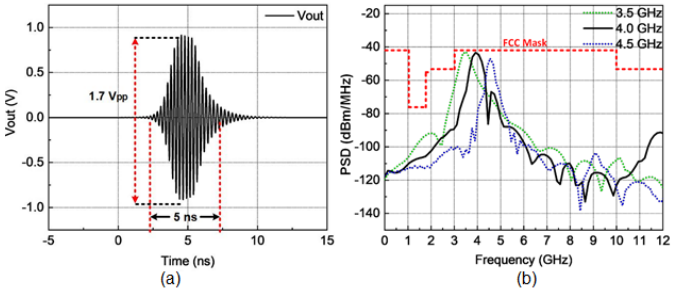

Fig. 8. (a) PA output @100 kbps (Zoomed view), (b) Power spectral density of 3.5 GHz, 4.0 GHz and 4.5 GHz transmit signal.

the control voltage V_{ctrl} from 800 mV to 1.4 V, the operating frequency of the VCO can vary from 3.5-4.5 GHz. The output signal of the PA is shown in Fig. 8 (a). The pulse width of the output signal is recorded as ∼5 ns with a maximum voltage of 1.7 V_{pp}. The gain of the proposed PA is simulated to be ∼6 dB for the frequency range of 3.5-4.5 GHz. From the output of the PA, the power spectral density (PSD) of the transmitted signal is also simulated. The PSD plot presented in Fig. 8(b) shows that the center frequency is at 4 GHz where the peak amplitude is -43.6 dBm/MHz with a -10 dB bandwidth of 700 MHz. The average power consumption of the transmitter is 105 pW for 1.8 V supply voltage and the energy efficiency of the transmitter is simulated to be 8.5 pJ/pulse at 100 kbps data rate. The on-chip amplifier, ADC, and transmitter consume a total of ∼280 μW.

IV. Conclusion

This paper presents a self-powered on-chip motion sensor, which acquires the motion detecting signal and transmits it wirelessly. The on-chip rectifier provides the DC supply voltages to the recording circuitry: amplifier, ADC, as well as to the transmitter. In the future, the full system can be implemented on a flexible substrate to remotely monitor motion activities of the body.

Acknowledgment

This material is based upon work supported by the National Science Foundation under Grant No. ECCS 1933502.

REFERENCES

[1] M. Ha, J. Park, Y. Lee and H. Ko, "Triboelectric generators and sensors for self-powered wearable electronics," Acs Nano, vol. 9, (4), pp. 3421-3427, 2015.

[2] T. J. Voss, V. Subbian and F. R. Beyette, "Feasibility of energy harvesting techniques for wearable medical devices," in 2014 36th Annual International Conference of the IEEE Engineering in Medicine and Biology Society, 2014, pp. 626-629.

[3] Y. Wang, Y. Yang and Z. L. Wang, "Triboelectric nanogenerators as flexible power sources," Npj Flexible Electronics, vol. 1, (1), pp. 10, 2017.

[4] J. Zhong, Y. Zhang, Q. Zhong, Q. Hu, B. Hu, Z. L. Wang and J. Zhou, "Fiber-based generator for wearable electronics and mobile medication," ACS Nano, vol. 8, (6), pp. 6273-6280, 2014.

[5] V. Misra, A. Bozkurt, B. Calhoun, T. Jackson, J. S. Jur, J. Lach, B. Lee, J. Muth, Ö Oralkan and M. Öztürk, "Flexible technologies for self-powered wearable health and environmental sensing," Proc IEEE, vol. 103, (4), pp. 665-681, 2015.

[6] T. Krupenkin and J. A. Taylor, "Reverse electrowetting as a new approach to high-power energy harvesting," Nature Communications, vol. 2, pp. 448, 2011.

[7] G. Chong, H. Ramiah, J. Yin, J. Rajendran, W. W. Ru, P. Mak and R. P. Martins, "CMOS Cross-Coupled Differential-Drive Rectifier in Subthreshold Operation for Ambient RF Energy Harvesting-Model and Analysis," IEEE Transactions on Circuits and Systems II: Express Briefs, 2019.

[8] G. Chong, H. Ramiah, J. Yin, J. Rajendran, P. Mak and R. P. Martins, "A Wide-PCE-Dynamic-Range CMOS Cross-Coupled Differential-Drive Rectifier for Ambient RF Energy Harvesting," IEEE Transactions on Circuits and Systems II: Express Briefs, 2019.

[9] N. T. Tasneem, S. R. Suri and I. Mahbub, "A low-power CMOS voltage boosting rectifier for wireless power transfer applications," in 2018 Texas Symposium on Wireless and Microwave Circuits and Systems (WMCS), 2018, pp. 1-4.

[10] R. S. Assaad and J. Silva-Martinez, "The recycling folded cascode: A general enhancement of the folded cascode amplifier," IEEE J Solid State Circuits, vol. 44, (9), pp. 2535-2542, 2009.

[11] M. Akbari, O. Hashemipour and A. Javid, "An ultra-low voltage, ultra-low power fully recycling folded cascode amplifier," in 2014 22nd Iranian Conference on Electrical Engineering (ICEE), 2014, pp. 514-518.

[12] M. Akbari, S. Biabanifard, S. Asadi and M. C. Yagoub, "Design and analysis of DC gain and transconductance boosted recycling folded cascode OTA," AEU-International Journal of Electronics and Communications, vol. 68, (11), pp. 1047-1052, 2014.

[13] X. Zhao, H. Fang and J. Xu, "DC gain enhancement method for recycling folded cascode amplifier in deep submicron CMOS technology," IEICE Electronics Express, vol. 8, (17), pp. 1450-1454, 2011.

[14] X. Zhao, H. Fang and J. Xu, "A transconductance enhanced recycling structure for folded cascode amplifier,"Analog Integr. Cir. Signal Proc., vol. 72, (1), pp. 259-263, 2012.

[15] X. Zhao, Y. Wang and L. Dong, "Super current recycling folded cascode amplifier with ultra-high current efficiency," Integration, vol. 62, pp. 322-328, 2018.

[16] C. Liu, S. Chang, G. Huang and Y. Lin, "A 10-bit 50-MS/s SAR ADC with a monotonic capacitor switching procedure," IEEE J Solid State Circuits, vol. 45, (4), pp. 731-740, 2010.

[17] P. Harpe, C. Zhou, X. Wang, G. Dolmans and H. de Groot, "A 30fJ/conversion-step 8b 0-to-10MS/s asynchronous SAR ADC in 90nm CMOS," in 2010 IEEE International Solid-State Circuits Conference-(ISSCC), 2010, pp. 388-389.

[18] T. Haapala, M. Pulkkinen, J. Salomaa and K. Halonen, "A 180-nW static power UWB IR transmitter front-end for energy harvesting applications," in 2017 IEEE International Symposium on Circuits and Systems (ISCAS), 2017, pp. 1-4.

[19] US Federal Communications Commission, FCC Revision of Part 15 of the Commission's Rules regarding Ultra-Wideband Transmission Systems: First Report and Order, 2002.

[20] F. U. Khan and M. U. Qadir, "State-of-the-art in vibration-based electrostatic energy harvesting - IOPscience," p. 28 pp, 2016.

[21] J. L. González, A. J. F. Rubio, and F. Moll, "Human Powered Piezoelectric Batteries to Supply Power to Wearable Electronic Devices," 2002.

[22] R. S. Suri, N. T. Tasneem and I. Mahbub, "Low-Power Highly Efficient Voltage-Boosting Rectifier for Wide-band Inductively-Coupled Power Telemetry," 2019 United States National Committee of URSI National Radio Science Meeting (USNC-URSI NRSM), Boulder, CO, USA, 2019, pp. 1-2.